

1 **Anionic Guests in Prismatic Cavities Generated by Enneanuclear Nickel Metallacycles**

2
3
4 Jordi Esteban,^{*,†} Mercè Font-Bardia,^{‡,§} and Albert Escuer^{*,†}

5
6
7
8
9
10
11
12
13
14
15
16 [†]Departament de Química Inorgànica, Universitat de Barcelona, Av. Diagonal 645, 08028 Barcelona,
17 Spain

18 [‡]Departament de Mineralogia, Cristal·lografia i Dipòsits Minerals, Universitat de Barcelona, Martí
19 Franqués s/n, 08028 Barcelona, Spain

20 [§]Unitat de Difracció de R-X, Centre Científic i Tecnològic de la Universitat de Barcelona (CCiTUB),
21 Universitat de Barcelona, Soléi Sabarís 1-3, 08028 Barcelona, Spain

22
23
24
25
26
27
28
29
30
31
32
33

34 **ABSTRACT**

35

36 The combination of polydentate aminated ligands with the 2-pyridyloxime-nickel-azide system leads to
37 series of clusters with unprecedented topologies. Among them, a remarkable family of {Ni₉}
38 metallacycles that are capable of selective encapsulation of azide/halide anions in a cryptand-like cavity
39 through hydrogen-bond interactions has been characterized.

40

41

42

43

44 INTRODUCTION

45

46 Anion binding and sensing is an expanding field within supramolecular chemistry, because of its
47 applications in anion exchange and transport, biomedical and environmental monitoring, molecular
48 recognition, and crystal engineering.¹ Among the different supramolecular strategies to synthesize this
49 receptors, chemical (anion) template² offers a rational and efficient approach to molecular and
50 supramolecular assemblies, but also allows the preparation of unusual topologies, such as rotaxanes,
51 helicates, and catenanes.³

52 Despite the fact that most anion receptors are preformed organic molecules,^{2a,4} the number of hosts that
53 incorporate metallic centers in its structure is increasing.⁵ Typical functions for metal centers in anion
54 hosts have been structure-organizing and binding groups but, furthermore, the positive charge of the
55 metal center contributes to a more favorable binding via columbic interaction, which is added to other
56 host-guest interactions. One of the most useful noncovalent host-guest interactions are hydrogen bonds,
57 because of their directionality and relative strength. In addition, the presence of nearby electron-
58 withdrawing metal centers can boost the hydrogenbond donor ability of the group and, consequently,
59 enhance the host-guest interaction.

60 Coordination of azide anion by the well-known (N₃)⁻ [BT-6H⁺] bis-trend hexaprotonated cryptand⁶
61 was established by the Lehn group in his seminal work in 1984. However, after this early work, the
62 number of X-ray characterized specific receptors for this anion is surprisingly reduced in comparison
63 with oxoanions or halides: in addition to the preformed [BT-6H⁺] cryptand in which the azide anion is
64 linked by six hydrogen bonds in a prismatic arrangement, only five preformed organic receptors⁷ and
65 one pseudo-spherical metallocage in which the interaction with the guest involves weak C-H...N
66 bonds,⁸ have been recently characterized.

67 Pyridyloximes have been extensively employed in recent years in cluster coordination chemistry,⁹
68 because of their coordinative versatility, that allows them to bridge up to four metallic centers and their
69 easy functionalization. Focusing on nickel derivatives, the chemistry of 2-pyridyloximes, (py)C{R}-
70 NOH, has yielded a large variety of topologies and nuclearities up to Ni₄.¹⁰ Combination of
71 pyridyloximes and μ -1,1-azido bridges has proven an adequate method to obtain high-spin ground states
72 and with SMM response in some cases.¹¹

73 In the search of new synthetic routes, we have combined aliphatic polydentate amines with the
74 nickel-oximate-azido system (Chart 1), and we report the syntheses and characterization (see details
75 and Scheme S1 in the Supporting Information) of the trinuclear complex
76 [Ni₃(Medpt)₂(py₂CNO)₂(N₃)₄](1·MeOH); the tetranuclear compounds [Ni₄(Medpt)₂(N₃)₄(dapdo)₂]
77 (2·MeOH), [Ni₄(dpt)₂(N₃)₄(py₂CNO)₄](3·2MeCN), and [Ni₄(Me₃dpt)₂(N₃)₄(pyC{ph}NO)₄]
78 (4·4MeCN); the pentanuclear complex [Ni₅(H₂O)₄(AcO)₂(N₃)₂(OH)₂(pyC{ph}NO)₄]
79 (5·5MeCN, H₂O); and a series of enneanuclear metallacycles with formula: (N₃)⁻
80 [Ni₉(dpt)₆(pyC{ph}NO)₆(N₃)₉](A)₂ (where A = NO₃⁻ (6·MeCN), BF₄⁻ (7·2H₂O), F⁻ (8·MeOH),
81 and Cl⁻ (9·H₂O)), (X)⁻ [Ni₉(dpt)₆(pyC{ph}NO)₆(N₃)₉](X)₂ (X = Br⁻ (10·H₂O) and I⁻ (11·2H₂O)),
82 and (N₃)⁻ [Ni₉(dpt)₆(py₂CNOH)₆(N₃)₉](ClO₄)₂ (12·2MeOH), in which py₂CNO⁻,
83 pyC{ph}NO⁻, and dapdo²⁻ are the deprotonated forms of dipyridylketoneoxime, phenyl-
84 pyridylketoneoxime and 2,6-diacetylpyridinedioxime, respectively, and dpt is dipropyltriamine.

85 This work focuses on two types of compounds derived from the new synthetic strategy of blending of 2-
86 pyridyloximates with aliphatic amines: (i) the complete description of series of low-nuclearity
87 complexes (Ni₃, Ni₄, and Ni₅); and (ii) the description of unprecedented series of nonanuclear
88 metallacrowns able to coordinate a variety of anions in a similar way to classic cryptands. An exhaustive
89 structural analysis of the {Ni₉} family has been carried out, and some comments about the system
90 selectivity are pointed out. Unfortunately, the labile bis-monodentate μ -1,3-azido bridge is broken in

91 solution as was proven by mass spectroscopy,¹² and then these complexes are only stable in solid state,
92 preventing the study of association constants. Finally, DC susceptibility measurements carried in the
93 2–300 K temperature range have been realized for all the reported topologies. Compounds 1, 6, and
94 9–11 were previously described in a short communication.¹²

95 .

96

97 **EXPERIMENTAL SECTION**

98

99 **Syntheses.** py2CNOH and pyC{ph}NOH ligands, as well as the aminated groups, were purchased from
 100 Sigma–Aldrich, Inc., and used without further purification. Nickel salts were purchased from
 101 Sigma–Aldrich, Inc., Fluka AG, and Strem Chemicals, Inc.

102 [Ni3(Medpt)2(py2CNO)2(N3)4]·MeOH (1). Compound 1, which is defined as
 103 [Ni3(Medpt)2(py2CNO)2(N3)4]·MeOH, was obtained in good yield via reaction in methanolic medium
 104 of py2CNOH ligand (199 mg, 1 mmol), [Ni2(Medpt)2(N3)4] (576 mg, 1 mmol), and triethylamine (202
 105 mg, 2 mmol). The resulting solution was left to slow evaporation and prismatic dark crystals appeared
 106 after a week. Anal. Calcd for C37H58N24Ni3O3 (1·MeOH): C, 41.8%; H, 5.5%; N, 31.6%. Found: C,
 107 40.9%; H, 5.3%; N, 31.5%.

108 [Ni4(Medpt)2(N3)4(dapdo)2]·MeOH (2). Compound 2, which is defined as
 109 [Ni4(Medpt)2(N3)4(dapdo)2]·MeOH, was obtained from the reaction of [Ni2(Medpt)2(N3)4] (576 mg,
 110 1 mmol), dapdoH2 ligand (178 mg, 1 mmol) and NEt3 (202 mg, 2 mmol) in 20 mL of MeOH. The
 111 mixture was stirred, filtered, and left for slow crystallization in a closed vial. Red prismatic crystals were
 112 collected a month later. Anal. Calcd for C32H56N24Ni4O4 (2): C, 35.7%; H, 5.2%; N, 31.2%. Found:
 113 C, 35.2%; H, 5.0%; N, 31.6%.

114 [Ni4(dpt)2(N3)4(py2CNO)4]·2MeCN (3) and [Ni4(Me3dpt)2(N3)4(pyC-{ph}NO)4]·4MeCN (4).
 115 Compounds 3 ([Ni4(dpt)2(N3)4(py2CNO)4]·2MeCN) and 4
 116 ([Ni4(Me3dpt)2(N3)4(pyC{ph}NO)4]·4MeCN) were synthesized from NiCl2·6H2O (474 mg, 2 mmol),
 117 dipropylene triamine (262 mg, 2 mmol) with py2CNOH (199 mg, 1 mmol); and Ni(BF4)2·6H2O (680
 118 mg, 2 mmol), Me3dpt (346 mg, 2 mmol) with pyC{ph}NOH (198 mg, 1 mmol), respectively, together
 119 with NaN3 (260 mg, 4 mmol) and NEt3 (202 mg, 2 mmol) in 20 mL of MeCN. The resultant mixtures
 120 were stirred, filtered, and left for slow evaporation. Red prismatic crystals were collected after a month.
 121 Anal. Calcd for C56H66N30Ni4O4 (3): C, 46.1%; H, 4.6%; N, 28.8%. Found: C, 45.5%; H, 4.8%; N,
 122 28.3%.

123 [Ni5(H2O)4(AcO)2(N3)2(OH)2(pyC{ph}NO)4]·5MeCN,H2O (5). Compound 5, which is defined as
 124 [Ni5(H2O)4(AcO)2(N3)2(OH)2(pyC-{ph}NO)4]·5MeCN,H2O, was obtained as red brick-shaped
 125 crystals from the slow evaporation of the resultant solution of Ni(AcO)2·4H2O (594 mg, 2 mmol),
 126 pyC{ph}NOH (199 mg, 1 mmol), Me3dpt (346 mg, 2 mmol), NaN3 (260 mg, 4 mmol), and NEt3 (202
 127 mg, 2 mmol) in 20 mL of MeCN. Anal. Calcd for C52H52N14Ni5O14 (5): C, 46.1%; H, 4.5%; N,
 128 28.8%. Found: C, 43.8%; H, 4.2%; N, 27.1%. (N3) ⊂ [Ni9(dpt)6(pyC{ph}NO)6(N3)9](NO3)2·MeCN
 129 (6). Compound 6, which is defined as (N3) ⊂ [Ni9(dpt)6(pyC{ph}NO)6(N3)9]-(NO3)2·MeCN, was
 130 synthesized via reaction of pyC{ph}NOH (198 mg, 1 mmol), Ni(NO3)2 (580 mg, 2 mmol), dipropylene
 131 triamine (162 mg, 2 mmol), NaN3 (260 mg, 4 mmol), and NEt3 (202 mg, 2 mmol) in 20 mL of
 132 acetonitrile. The solution was left to evaporate slowly and brown prisms were obtained after a week.
 133 Anal. Calcd for C108H156N62Ni9O12 (6): C, 42.6%; H, 5.2%; N, 28.5%. Found: C, 42.4%; H, 5.2%;
 134 N, 29.0%.

135 (N3) ⊂ [Ni9(dpt)6(pyC{ph}NO)6(N3)9](A)2 (A = BF4 (7), F (8), and Cl (9)); (X) ⊂
 136 [Ni9(dpt)6(pyC{ph}NO)6(N3)9](X)2·nH2O (X = Br (10), I (11)); and (N3) ⊂
 137 [Ni9(dpt)6(py2CNO)6(N3)9](ClO4)2·2MeOH (12). Compounds 7, 8, and 9 (defined as (N3) ⊂
 138 [Ni9(dpt)6(pyC{ph}-NO)6(N3)9](A)2 (where A = BF4 (7), F (8), and Cl (9)), 10 and 11 (defined as (X)
 139 ⊂ [Ni9(dpt)6(pyC{ph}NO)6(N3)9](X)2·nH2O (where X = Br (10) and I (11)), and 12 (which is defined
 140 as (N3) ⊂ [Ni9(dpt)6(py2CNO)6(N3)9](ClO4)2·2MeOH) were obtained following the same procedure
 141 as that for compound 6 in methanolic solution, starting from the corresponding nickel salt and using the
 142 py2CNOH ligand instead of pyC{ph}NOH for 12. Dark prisms crystallized one week later. Anal. Calcd
 143 for C108H160B2F8N60Ni9O8 (7·2H2O): C, 41.5%; H, 5.1%; N, 26.8%. Found: C, 37.5%; H, 4.7%; N,

144 23.7%. Anal. Calcd for C₁₀₈H₁₅₈Cl₂N₆₀Ni₉O₇ (9·H₂O): C, 43.1%; H, 5.3%; N, 28.0%. Found: C,
145 42.3%; H, 5.1%; N, 28.1%. Anal. Calcd for C₁₀₈H₁₅₈Br₃N₅₇Ni₉O₇ (10·H₂O): C, 41.4%; H, 5.1%; N,
146 25.5%. Found: C, 41.5%; H, 5.2%; N, 25.7%. Anal. Calcd for C₁₀₈H₁₆₀I₃N₅₇Ni₉O₈ (11·2H₂O): C,
147 39.4%; H, 4.9%; N, 24.4%. Found: C, 39.8%; H, 5.0%; N, 24.1%. Anal. Calcd for
148 C₁₀₄Cl₂H₁₅₄I₃N₆₆Ni₉O₁₆ (12·2MeOH): C, 38.8%; H, 4.8%; N, 29.2%. Found: C, 39.8%; H, 5.0%;
149 N, 28.1%.

150 All samples were obtained in good yield (~40%) as well-formed large crystals. The yield of the
151 reactions is greater than 40%, but it was not quantified, because the collection of the samples for
152 instrumental measures was limited to the well-formed first crystalline fraction.

153 **Physical Measurements.** Magnetic susceptibility measurements were carried out on polycrystalline
154 samples with a MPMS5 Quantum Design susceptometer working in the range of 30–300 K under an
155 external magnetic field of 0.3 T and under a magnetic field of 0.03 T in the temperature range of 30–2
156 K, to avoid saturation effects. Diamagnetic corrections were estimated from the Pascal tables. Infrared
157 spectra (4000–400 cm⁻¹) were recorded from KBr pellets on a Bruker IFS-125 FT-IR
158 spectrophotometer.

159 **X-ray Crystallography.** Details of crystal data, data collection, and refinement are given in Tables S1,
160 S2, and S3 in the Supporting Information, whereas experimental details for all compounds are provided
161 in Tables S4–S8 and Figures S1–S5 in the Supporting Information. X-ray data were collected on a
162 MAR345 diffractometer with an image plate detector for compounds 1, 2, 3, and 7, on a Bruker Kappa
163 ApexII CCD diffractometer for compounds 6 and 8–12, on a Supernova system for compound 4, and on
164 a Bruker D8 Venture system for 5, with Mo K α radiation ($\lambda = 0.71073$ nm). The structures were solved
165 by direct methods using SHELXS computer program¹³ and refined using a full-matrix least-squares
166 method with the SHELXS97 computer program.¹⁴

167 All data can be found in the supplementary crystallographic data for this paper in CIF format with
168 CCDC Nos. 859276–859278, 876039–876040, and 948759–948765. These data can be obtained free of
169 charge from The Cambridge Crystallographic Data Centre via www.ccdc.cam.ac.uk/data_request/cif.
170 Plots for publication were generated with ORTEP3 for Windows and plotted with Pov-Ray programs.¹⁵

171

172 **RESULTS AND DISCUSSION**

173

174 **Comments to the Syntheses.** Our initial synthetic strategy was to employ, as the nickel source, the
175 neutral dinuclear complex $[\text{Ni}_2(\text{Medpt})_2(\text{N}_3)_4]$ (previously reported by us¹⁶), which contains the
176 aminated ligand Medpt and preformed μ -1,1-azido bridges. Our objective was to avoid the presence of
177 counteranions other than azide, in order to reach the syntheses of ferromagnetic clusters containing μ -
178 1,1-azido bridges. As result of the reaction of $[\text{Ni}_2(\text{Medpt})_2(\text{N}_3)_4]$ with a variety of pyridyloximes
179 (Chart 1), neutral complexes 1 and 2 were characterized.

180 In light of the structural data, we realized that, despite the presence of terminal azido ligands, the
181 nuclearity of cluster 1 is limited to the low nuclearity Ni_3 entity. This complex is neutral and in order to
182 bind these terminal azido ligands, additional counteranions were needed to balance the resulting positive
183 charge. Thus, the same reaction was tried from $[\text{Ni}_2(\text{Medpt})_2(\text{N}_3)_4]$ and $[\text{Ni}_2(\text{dpt})_2(\text{N}_3)_4]$ adding small
184 amounts of sodium nitrate and then, enneanuclear complex 6 was obtained. Further synthetic work
185 revealed that the $\{\text{Ni}_9\}$ ring 6 can be obtained in high yield from the direct reaction of nickel nitrate, the
186 aminated ligand, and sodium azide, and the direct synthesis was assumed to be preferable, as described
187 in the Syntheses section for 6–12.

188 From this result, similar reactions with series of different starting reagents were performed in order to
189 elucidate three questions: (i) the effect of the anion on the final structure, (ii) the influence of the
190 aminated ligand, and (iii) the ability of this system to encapsulate spherical anions as halides.

191 In addition to the medium nuclearity compounds 3–5, reaction with BF_4^- or ClO_4^- salts gave
192 structures similar to that of the nitrate complex 6 (complexes 7 and 12). Reaction starting from NiII
193 halides yields the same structure for fluoride and chloride (8 and 9) but successful incorporation of the
194 halide anion as a guest was achieved starting from NiBr_2 and NiI_2 salts (complexes 10 and 11).
195 Complex 5 is the only one that does not incorporate the tridentate amine in its structure, which gives
196 proof of the stability of the bowtie topology^{11,17} for the oximato/azide/carboxylato blend of ligands and
197 is closely related to $[\text{Ni}_5(\text{MeOH})_4(\text{AcO})_2(\text{N}_3)_2(\mu_3\text{-N}_3)_2(\text{pyC}\{\text{ph}\}\text{NO})_4]$ which contains a $\mu_3\text{-N}_3$
198 ligand instead the $\mu_3\text{-OH}$ central donor.¹¹

199 **Description and Magnetic Study.** Plots of the structure of the neutral complexes 1–5 are shown in
200 Figure 1. Labeled plots and selected structural parameters are given in Figures S1–S5 and Tables S4–S8
201 in the Supporting Information.

202 Compound 1 consists of a neutral angular trinuclear unit linked by double oximato/ μ -1,1-azide bridges
203 (Figure 1). The central Ni-atom exhibits a NiN_6 coordination sphere from two py_2CNO^- ligands (each
204 one bound by two of their N atoms) and the two N_3^- binding groups whereas external Ni atoms present
205 a NiN_5O environment that comes from one Medpt ligand, which acts as tridentate ligand in mer
206 coordination, one bridging and one terminal azide group and finally an O-oximato ligand. Ni–N–Ni
207 bond angles are relatively large with values of $112.9(1)^\circ$ and $112.2(1)^\circ$ and the Ni–O–N–Ni torsion
208 angles are $17.0(3)^\circ$ and $4.3(3)^\circ$.

209 Complex 2 consists of two dinuclear subunits linked by means of μ -1,3-azido bridges. Each subunit is
210 formed by two Ni atoms (one of them linking one tridentate Medpt ligand and the other linking one
211 dapdo_2^- dioximate), bridged as in the previous complex by a double oximato/ μ -1,1- N_3^- bridge,
212 which exhibits similar Ni–N–Ni and Ni–O–N–Ni angles of $112.36(9)^\circ$ and $14.6(2)^\circ$, respectively. The Ni
213 atom linked to the Medpt ligand shows an octahedral environment, whereas the Ni atom coordinated to
214 the dapdo_2^- ligand exhibits a square planar environment in agreement the high field induced by the
215 fully deprotonated dapdo_2^- dioximate.¹⁸ Weak Ni–N(azide) interaction with bond distance of $2.820(3)$
216 Å (Figure 1) and a set of hydrogen bonds link the two subunits to give the tetranuclear system (see
217 details given in Figure S2 in the Supporting Information).

218 A view of the core of compound 3 is illustrated in Figure 1. The centrosymmetric tetranuclear complex
219 3 can be described as being similar to two oximato/ μ -1,1-N3 – bridged dinuclear subunits (similar to
220 compound 1), linked together by a double oximato bridge. As in the previous case, the central Ni atoms
221 are coordinated by the N atoms of the pyridyloximate ligands, whereas the peripheral nickels bind the
222 aminated tridentate ligands. Ni–N–Ni bond angle is 111.4(1)° and Ni–O–N–Ni torsion angles are
223 20.0(2)° and 24.0(2)°. The different ligands employed in 3 (Medpt and py2CNO–) and 4 (Me3dpt and
224 pyC{ph}NO–) are not relevant from structural point of view and the two complexes show the same
225 topology and very close bond parameters (see Tables S6 and S7 in the Supporting Information).

226 The neutral core of the centrosymmetric pentanuclear compound 5 can be described as a bowtie
227 arrangement of five NiIII ions, or, in other words, it is similar to two isosceles triangles sharing one
228 vertex (Figure 1). Each triangle is μ 3–OH centered with the OH bridging group being displaced
229 0.725(2) Å out of the plane formed by the three Ni atoms. Two sides of the triangles are defined by
230 single oximato bridges between the central and the peripheral nickel atoms whereas the external NiIII
231 atoms are bridged by one syn–syn acetate ligand and one μ 1,1-N3 – bridging group. Ni–N–Ni bond
232 angle is 90.51(7)° and Ni–O–N–Ni torsion angles are quasiplanar (1.2(2)° and 3.4(2)°).

233 Central Ni(1) atom presents a NiO6 environment that proceeds from the two μ 3-OH and four O-oximato
234 ligands. Parallely, peripheral Ni(2,3) atoms exhibit a NiN3O3 environment that arises from one
235 pyridyloxime ligand linked by its two N atoms, the μ -1,1 azide, the μ 3-OH central group, one syn-syn
236 acetate ligand and finally one coordinated water molecule. Four intramolecular hydrogen bonds between
237 the water molecules and the oxygen atom of the oximate groups help to stabilize the structure (Figure S5
238 in the Supporting Information). The crystallization water molecule establish intermolecular hydrogen
239 bonds involving the coordinated water molecules giving a supramolecular 1D arrangement.

240 χ MT vs. T plot for complexes 1, 3, and 5 are shown in Figure 2 (3 and 4 show quasi identical bond
241 parameters and 2 contains diamagnetic square planar nickel atoms and then, 2 and 4 were not measured).
242 Complex 1 is ferromagnetically coupled; 3 shows an overall antiferromagnetic response whereas 5
243 exhibits the typical χ MT minimum characteristic of ferromagnetic behavior.

244 The experimental data was fitted according to the interaction patterns shown in Chart 2A for 1, Chart 2B
245 for 3, Chart 2C for 5, and the derived Hamiltonians:

246

$$247 \quad H = -J_1 (S_1 \cdot S_2 + S_1 \cdot S_3) \text{ for (1)}$$

$$248 \quad H = -J_1 (S_1 \cdot S_2 + S_3 \cdot S_4) - J_2 (S_2 \cdot S_3) \text{ for (3)}$$

$$249 \quad H = -J_1 (S_1 \cdot S_2 + S_1 \cdot S_3 + S_1 \cdot S_4 + S_1 \cdot S_5)$$

$$250 \quad -J_2 (S_2 \cdot S_3 + S_4 \cdot S_5) \text{ for (5)}$$

251

252 Compounds 1 and 5 were fitted with the derived analytical equations, whereas, for 3, the CLUMAG
253 program19 was employed. Best-fit parameters were $J_1 = +9.8(1) \text{ cm}^{-1}$ and $g = 2.155(3)$ for the trimeric
254 complex 1, $J_1 = +10.2 \text{ cm}^{-1}$, $J_2 = -28.7 \text{ cm}^{-1}$, $g = 2.120$ and $R = 3.56 \times 10^{-5}$ ($R = (\chi_{\text{MTcalc}} -$
255 $\chi_{\text{MTexp}})^2 / (\chi_{\text{MTexp}})^2$) for the tetranuclear complex 3 and $J_1 = -24.3(1) \text{ cm}^{-1}$, $J_2 = +23.1(4) \text{ cm}^{-1}$ and
256 $g = 2.209(1)$ for the pentanuclear complex 5.

257 The double oximato/ μ -1,1-azide bridges between two NiIII cations have been observed as fragments of
258 larger clusters and overall ferromagnetic interaction was proposed for these fragments. However,
259 complex 1 provides the unambiguous assignation of ferromagnetic coupling for this combination of
260 superexchange pathways and it is confirmed by the value of J_1 obtained for complex 3, which is in full

261 agreement with 1. From the sign and magnitude of the calculated coupling constants, the proposed
262 ground states are $S = 3$ for 1, $S = 0$ for 3, and $S = 3$ for 5.

263 Compounds 6–9, and 12, present the same structure except for the substitution $\text{pyC}\{\text{ph}\}\text{CNOH}$ for
264 $\text{py}2\text{CNOH}$ in 12 and the variation of the corresponding anion in each case. Thus, we only describe the
265 structural details of 6 to avoid repetitive descriptions.

266 This compound can be described to be similar to three trimeric angular subunits linked by μ -1,3-azido
267 bridges generating a $\{\text{Ni}_9\}$ ring, with $\text{Ni}(1)\text{--Ni}(6)\text{--Ni}(2)$ bond angle of $110.89(7)^\circ$ and
268 $\text{Ni}(1)\text{--Ni}(2)\text{--O}(1)\text{--Ni}(2)$ torsion angle of $17.6(2)^\circ$. Coordination of two oximate ligands to $\text{Ni}(1)$ and the
269 tridentate amines to $\text{Ni}(2)$ are fully comparable with complex 1 and thus, the $\{\text{Ni}_9\}$ ring can be
270 structurally described as a trimer of trimers (see Figure 3). The μ -1,3 bridges show $\text{Ni}(2)\text{--N}(9)\text{--N}(10)$
271 bond angles of $128.2(2)^\circ$ and a quasi planar $\text{Ni}\text{--NNN}\text{--Ni}$ torsion angle of $171.8(1)^\circ$.

272 The shorter linkage sequence $\{\text{--Ni}(\mu 1,1\text{N}3)\text{--Ni}(\mu 1,1\text{N}3)\text{--Ni}(\mu 1,3\text{N}3)\text{--}\}_3$ determines a 24-
273 membered ring containing six monatomic bridges (μ -1,1-azide) and three triatomic bridges (μ -1,3-
274 azide), which gives the larger azido metallacrown reported to date.

275 The ring is not planar due to the arrangement of the μ -1,3- azido bridges, exhibiting a zig-zag ring
276 conformation that generates a large internal prismatic cavity functionalized by six --NH_2 groups from
277 the six dpt ligands (see Figure 4). These- NH_2 functions establish six hydrogen bonds with one azide
278 anion trapped inside the cavity along the C3 axis. $\text{N}(3)\text{--H}(3\text{a})\cdots\text{N}(11)$ distance is $3.037(2)$ Å. In
279 addition, a set of hydrogen bonds involving the $\text{N}(6)$ atom from the μ -1,1-azide bridges and the
280 aminated functions ($\text{N}(3)\text{--H}(3\text{b})\cdots\text{N}(6)$, $3.117(2)$ Å and $\text{N}(5)\text{--H}(5\text{b})\cdots\text{N}(6)$, $3.016(3)$ Å) helps to
281 stabilize the zig-zag conformation of the ring. Relevant intermolecular interactions were not found.

282 Finally, the three positive charges on the ring are compensated by the guest azide anion and two ionic
283 nitrates.

284 Compounds 10 and 11 exhibit the same metallacrown structure than the previous ones; however, in
285 these cases, the $\{\text{Ni}_9\}$ rings encapsulate a bromide (10) or iodide (11) anion, also stabilized in this
286 position by six hydrogen bonds. As in the above complexes 6–9, and 12, the cavity is a trigonal prism
287 and the main bond parameters related with the bridging azide and oximate ligands are fully comparable,
288 indicating that the conformation of the ring is poorly flexible (Figure 5). Detailed parameters for the
289 hydrogen bonds are reported in Table S9 in the Supporting Information.

290 On basis of the common bond parameters in the bridging region for all the enneanuclear rings (Table 1),
291 magnetic measurements were performed on a representative complex encapsulating one azide and one
292 halide anion. χ_{MT} vs. T plot for complexes 6 and 10 are shown in Figure 6. Both of them exhibit a very
293 similar shape and values indicating that, as should be expected, the guest anion does not influence the
294 superexchange interactions.

295 The experimental data was fitted with the CLUMAG program,¹⁹ according to the interaction pattern
296 shown in Chart 2D and the derived Hamiltonian:

297

$$298 \quad H = -J_1 (S_9 \cdot S_1 + S_1 \cdot S_2 + S_3 \cdot S_4 + S_4 \cdot S_5 + S_6 \cdot S_7 + S_7 \cdot S_8)$$

$$299 \quad -J_2 (S_2 \cdot S_3 + S_5 \cdot S_6 + S_8 \cdot S_9)$$

300

301 Best-fit parameters were $J_1 = +9.9 \text{ cm}^{-1}$, $J_2 = -62.5 \text{ cm}^{-1}$, $g = 2.289$, and $R = 1.25 \times 10^{-5}$ for 6 and J_1
302 $= +8.9 \text{ cm}^{-1}$, $J_2 = -53.5 \text{ cm}^{-1}$, $g = 2.211$, and $R = 1.57 \times 10^{-5}$ for 10. As expected from the similar
303 bond parameters of the double oximate/ μ -1,1-azide bridges, J_1 gives very close values to complexes 1

304 and 3. The sign and magnitude of J_2 is indicative of strong antiferromagnetic coupling, which lies in the
305 expected range²⁰ of values for a single μ -1,3-azido bridge with torsion angles of $\sim 175^\circ$ and Ni–N–N
306 bond angles close to 129° . The lower AF interaction for 10 can be attributed to the larger Ni–N bond
307 distance.

308 It should be emphasized that the coupling constants ($-J_1 - J_1 - J_2$)³ alternating with ferromagnetic J_1
309 and antiferromagnetic J_2 in a closed ring is unusual from a magnetic point of view. The strong AF
310 interaction J_2 cancels three pairs of spins but remain three $S = 1$ corners leading to a situation similar to
311 a NiIII triangle with diamagnetic $S = 0$ ground state, despite the odd number of spins (see Figure S6 in
312 the Supporting Information).

313 **Host–Guest Interactions.** Synthesis by self-assembly of the metallacrowns 6–12 is the result of the
314 subtle combination of several factors as charge balance, anionic effects, guest coordination and
315 hydrogen-bond interactions, which lead to the stabilization of this unusual supramolecular system. The
316 detailed analysis of these factors will be the subject of this section.

317 **Anion Effect.** The reaction of NiIII, tridentate amines, and 2- pyridyloximes without other anions in the
318 reaction medium than azido or oximate lead to neutral low nuclearity systems (Ni₃, Ni₄), which contain
319 the nickel centers bonded by double azido/oximate bridges. In contrast, the presence in the reaction
320 medium of a large variety of anions stabilizes the cationic nonanuclear metallacrowns 6–12
321 independently of the shape or size of the anions (NO₃⁻, BF₄⁻, ClO₄⁻, F⁻, Cl⁻, Br⁻, I⁻). The structure
322 of the metallacrowns 6–12 shows an evident relationship with trimeric complex 1 and they can be
323 described as “trimers of trimers”, which are linked by μ -1,3-azido bridges. Two factors emerge as
324 driving force for these reactions: on one hand, counteranions are necessary to balance the positive
325 charge of the ring, and on the other hand, the reaction needs a small anion (azide or halide) to give a
326 template assembly around it. The anionic guest and the counteranion become equally crucial to
327 determine the stability and topology of the enneanuclear metallacrowns.

328 Although Scheme 1 does not correspond to one real reaction, it illustrates the “stoichiometric”
329 relationship and the anion role between trinuclear complex 1 and enneanuclear complexes 6–9, and 12,
330 which contain one azide as an anionic guest.

331 **Azide as a Guest.** Compounds 6–9, and 12, coordinate the guest azide in a manner similar to that of
332 Lehn’s [BT-6H⁺] cryptand₆ (trigonal prismatic arrangement). This arrangement arises from six
333 hydrogen bonds established between six –NH₂ amino functions of the dpt ligands. The trigonal prisms
334 and even their distortions are surprisingly similar between the cryptand and the {Ni₉} rings, being the
335 main difference the degree of pyramidalization of the hydrogen bonds, which determines the bases of
336 the prisms (see Chart 3 and Table 2).

337 Analysis of the above data points out that the prismatic cavity is practically identical in all 6–12 cases.
338 Comparison with compound A shows that, although the cavity is clearly compressed in complexes 6–9,
339 and 12, the N–H \cdots N distances serve as evidence that the hydrogen bonds are equally effective in the
340 cryptand than in the {Ni₉} metallacrowns.

341 **Halides as Guest.** The [BT-6H⁺] cryptand is able to coordinate azido anions but also spherical anions as
342 halides. The highly flexible cryptand can rearrange its conformation by rotation in opposite sense of
343 their two moieties along its main edge and then generate an octahedral environment that fits spherical
344 guests more adequately.⁶ The reported {Ni₉} metallacrown is much more rigid and unable to change its
345 conformation.

346 However, the compressed prisms 6–9, and 12, show distances to the centroid of the cavity that are only
347 slightly larger than those found in (Br)[BT-6H⁺] (see Table 2), suggesting that halides could fit into
348 these prismatic cavities. This possibility was explored and complexes 10 and 11, containing one
349 bromide and one iodide guest in the unprecedented prismatic trigonal coordination (see Chart 3) were

350 successfully characterized showing that the shape of the cavity is not a determinant factor. In contrast,
351 reactions with nickel fluoride or chloride yielded the above-described complexes 8 and 9 in which the
352 smaller halides act only as counteranions and the cavity is occupied by one guest azide, evidencing that
353 the main factor involved with encapsulating the halides is their size.

354 Tridentate Amines Role. The tridentate aminated ligands establish a pack of six hydrogen bonds with
355 both central azide and halide guest anions, but the role of these ligands can be considered not only to
356 trap the central anion, but also to stabilize the {Ni9} ring. As it can be seen in Figure 7, the -NH₂
357 functions pointing to the center of the cavity link the guest anion with one of their H atoms, whereas
358 they establish another hydrogen bond employing their second H atom with the N(6) atom of the μ -1,1-
359 azido ligand. N(6) is also the receptor of a second hydrogen bond from the -NH₂ function in trans to the
360 inner -NH₂ group. Thus, the mer coordination of the ligand becomes essential to stabilize the entire
361 ring, pointing out that dpt is the optimal choice to generate these types of rings.

362 As experimental proof, the change of dpt ligand by N,N',N''- Me₃dpt, which is unable to establish some
363 of the hydrogenbond interactions, stabilizes complex 4 instead of the {Ni9} ring. Equally, experiments
364 trying the substitution of the dpt tridentate amine by the bidentate N-Meen (N-methylethylenediamine),
365 capable of establishing hydrogen-bond interactions with the central anion host but not with the nearby μ -
366 1,1-azide ligands leads to completely different topologies and nuclearities. 10c

367 Selectivity. One should remember that these complexes are not stable in solution and the selectivity
368 considerations concern the complexes in solid state exclusively. As has been proven, the {Ni9} ring is
369 able to encapsulate one azide/halide anion. However, it is noteworthy that, in all reactions involving
370 6–12, there exists a competition between the azide, which is always present in the reaction medium, and
371 the corresponding Ni²⁺ counterion (NO₃⁻, BF₄⁻, ClO₄⁻, or the halides) to fill the guest site.
372 Tetrahedral anions as BF₄⁻ or ClO₄⁻ can coordinate in prismatic environments but they require larger
373 cavities to fit adequately,²¹ and their inclusion in the {Ni9} cavity should be discarded as well for the
374 smaller halides (F, Cl⁻) for which the rigid cavity is too large to give effective hydrogen bonds. Thus,
375 experimental results indicate that the encapsulation inside the {Ni9} metallacrown is controlled by the
376 size of the cavity and that Br⁻ and I⁻ ions are preferred to the N₃⁻ species.

377

378 **CONCLUSIONS**

379

380 Tridentate amines and 2-pyridyloximate blend of ligands have been demonstrated to be adequate for the
381 syntheses of new and unprecedented topologies in oximate chemistry, such as compound 1, which
382 provided unambiguous experimental evidence of the ferromagnetic interaction promoted by double
383 oximate/azide bridges. Also, a series of Ni₃, Ni₄, and Ni₅ complexes have been synthesized, as well as
384 a family of selfassembled cryptand-like {Ni₉} rings that are able to selectively encapsulate azide/halide
385 anions, by reaction of different Ni²⁺ salts, azide, and dipyridylketoneoximate or
386 phenylpyridylketoneoximate ligands.

387 The azide/halide coordination takes place around six hydrogen bonds and generates a quiral helical
388 arrangement of the cavity of the {Ni₉} ring. N₃⁻, Br⁻, and I⁻ adequately fit the cavity size, excluding
389 other larger or smaller anions. The mer coordination of the aminated tridentate ligand determines the
390 stabilization of the {Ni₉} rings by means of a set of additional hydrogen bonds involving the two -NH₂
391 functions.

392

393

394 **AUTHOR INFORMATION**

395

396 **Corresponding Author**

397 *E-mail: albert.escuer@qi.ub.es.

398

399 **Notes**

400 The authors declare no competing financial interests.

401

402 **ACKNOWLEDGMENTS**

403

404 Funding from the CICYT (Project No. CTQ2012-30662) are acknowledged. A.E. is thankful for
405 financial support from the Excellence in Research ICREA-Academia Award.

406

407 **REFERENCES**

408

- 409 (1) (a) Gale, P. A.; Gunnlaugsson, T. *Chem. Soc. Rev.* 2010, 39, 3595. (b) Steed, J. *Chem. Soc.*
410 *Rev.* 2009, 38, 506. (c) Sessler, J. L.; Gale, P. A.; Cho, W.-S. *Anion Receptor Chemistry*; Royal
411 Society of Chemistry: Cambridge, U.K., 2006. (d) Kang, S. O.; Begum, R. A.; Bowman-James,
412 K. *Angew. Chem., Int. Ed.* 2006, 45, 7882. (e) Bowman-James, K. *Acc. Chem. Res.* 2005, 38,
413 671.
- 414 (2) (a) Ballester, P. *Chem. Soc. Rev.* 2010, 39, 3810. (b) Lawrance, G. A. *Chem. Rev.* 1986, 86, 17.
415 (c) Saalfrank, R. W.; Demleitner, B.; Glaser, H.; Maid, H.; Bathelt, D.; Hampel, F.; Bauer, W.;
416 Teichert, M. *Chem.-Eur. J.* 2002, 8, 2679. (d) Albrecht, M.; Janser, I.; Meyer, S.; Weis, P.;
417 Frohlich, R. *Chem. Commun.* 2003, 2854. (e) Glasson, C. R. K.; Meehan, G. V.; Clegg, J. K.;
418 Lindoy, L. F.; Turner, P.; Duriska, M. B.; Willis, R. *Chem. Commun.* 2008, 1190. (f)
419 Custelcean, R.; Bosano, J.; Bonnesen, P. V.; Kertesz, V.; Hay, B. P. *Angew. Chem., Int. Ed.*
420 2009, 48, 4025. (g) Bryantsev, V. S.; Hay, B. P. *J. Am. Chem. Soc.* 2006, 128, 2035.
- 421 (3) Diederich, F., Slang, P. J., Eds. *Templated Organic Synthesis*; Wiley-VCH: Weinheim,
422 Germany, 2000. (4) Kang, S. O.; Llinares, J. M.; Day, V. W.; Bowman-James, K. *Chem.*
423 *Soc. Rev.* 2010, 39, 3980.
- 424 (5) (a) Beer, P. D.; Gale, P. A. *Angew. Chem., Int. Ed.* 2001, 40, 486. (b) Rice, C. R. *Coord. Chem.*
425 *Rev.* 2006, 250, 3190. (c) Pérez, J.; Riera, L. *Chem. Soc. Rev.* 2008, 37, 2658. (d) Fabbrizzi, L.;
426 Poggi, A. *Chem. Soc. Rev.* 2013, 42, 1861.
- 427 (6) Dietrich, B.; Guilhem, J.; Lehn, J. M.; Pascard, C.; Sonveaux, E. *Helvet. Chim. Acta* 1984, 67,
428 91.
- 429 (7) (a) Kim, N.-K.; Chang, K.-J.; Moon, D.; Lah, M. S.; Jeong, K.-S. *Chem. Commun.* 2007, 3401.
430 (b) Kang, S. O.; Day, V. W.; Bowman-James, K. *Inorg. Chem.* 2010, 49, 8629. (c) Serpell, C. J.;
431 Cookson, J.; Thompson, A. L.; Beer, P. D. *Chem. Sci.* 2011, 2, 494. (d) Wang, X.; Jia, C.;
432 Huang, X.; Wu, B. *Inorg. Chem. Commun.* 2011, 14, 1508. (e) Bushmarinov, I. S.; Nabiev, O.
433 G.; Kostyanovsky, R. G.; Antipina, M. Y.; Lyssenko, K. A. *Cryst. Eng. Commun.* 2011, 13,
434 2930.

- 435 (8) Amendola, V.; Boiocchi, M.; Colasson, B.; Fabbrizzi, L.; Rodriguez-Douton, M. J.; Ugozzoli, F.
436 *Angew. Chem., Int. Ed.* 2006, 45, 6920.
- 437 (9) (a) Milios, C. J.; Stamatatos, T. C.; Perlepes, S. P. *Polyhedron* 2006, 25, 134. (b) Tasiopoulos,
438 A. J.; Perlepes, S. P. *Dalton Trans.* 2008, 5537.
- 439 (10) (a) Stamatatos, T. C.; Abboud, K. A.; Perlepes, S. P.; Christou, G. *Dalton Trans.* 2007, 3861. (b)
440 Stamatatos, T. C.; Escuer, A.; Abboud, K. A.; Raptopoulou, C. P.; Perlepes, S. P.; Christou, G.
441 *Inorg. Chem.* 2008, 47, 11825. (c) Esteban, J.; Alcazar, L.; Torres-Molina, M.; Monfort, M.;
442 Font-Bardia, M.; Escuer, A. *Inorg. Chem.* 2012, 51, 5503.
- 443 (11) Papatriantafyllopoulou, C.; Stamatatos, T. C.; Wernsdorfer, W.; Teat, S. J.; Tasiopoulos, A. J.;
444 Escuer, A.; Perlepes, S. P. *Inorg. Chem.* 2010, 49, 10486.
- 445 (12) Escuer, A.; Esteban, J.; Font-Bardia, M. *Chem. Commun.* 2012, 48, 9777.
- 446 (13) Sheldrick, G. M. SHELXS←A Computer Program for Determination of Crystal Structures;
447 University of Göttingen: Göttingen, Germany, 1997.
- 448 (14) Sheldrick, G. M. SHELX97←A Computer Program for Determination of Crystal Structures;
449 University of Göttingen: Göttingen, Germany, 1997.
- 450 (15) Farrugia, L. J. *J. Appl. Crystallogr.* 1997, 30, 565 (Ortep-3 for Windows).
- 451 (16) Escuer, A.; Vicente, R.; Ribas, J.; Solans, X. *Inorg. Chem.* 1995, 34, 1793.
- 452 (17) Esteban, J.; Ruiz, E.; Font-Bardia, M.; Calvet, T.; Escuer, A. *Chem.-Eur. J.* 2012, 18, 3637.
- 453 (18) (a) Escuer, A.; Esteban, J.; Aliaga-Alcalde, N.; Font-Bardia, M.; Calvet, T.; Roubeau, O.; Teat,
454 S. J. *Inorg. Chem.* 2010, 39, 2259. (b) Escuer, A.; Esteban, J.; Roubeau, O. *Inorg. Chem.* 2011,
455 50, 8893. (c) Esteban, J.; Escuer, A.; Font-Bardia, M.; Roubeau, O.; Teat, S. J. *Polyhedron*
456 2013, 52, 339.
- 457 (19) Gatteschi, D.; Pardi, L. *Gazz. Chim. Ital.* 1993, 123, 231 (CLUMAG program).
- 458 (20) Escuer, A.; Vicente, R.; Ribas, J.; El Fallah, M. S.; Solans, X.; Font-Bardia, M. *Inorg. Chem.*
459 1994, 33, 1842.
- 460 (21) Paul, R. L.; Bell, Z. R.; Jeffery, J. C.; McCleverty, J. A.; Ward, M. D. *Proc. Natl. Acad. Sci.*
461 U.S.A. 2002, 99, 4883..

462 **Legends to figures**

463

464 **Chart 1.** Pyridyloximate and Tridentate Aminated Ligands Discussed in the Text

465

466 **Figure 1.** View of the molecular structure of complexes 1, 2, 3, and 5. The weak axial azido–nickel
467 interaction in compound 2 is depicted in orange color. Color key: O, red; N, blue; C, black; octahedral
468 NiII, green; and square planar NiII, orange.

469

470 **Figure 2.** χ_{MT} vs T plot for complexes 1 (squares, \square), 3 (circles, \circ) and 5 (triangles, \triangle). Solid lines
471 show the best fit obtained.

472

473 **Chart 2.** Interaction Pattern with the Spin and Coupling Constant Labels for Topologies (A) 1, (B) 3,
474 (C) 5, and (D) Metallocrowns 6 and 10a

475

476 **Figure 3.** (Top) View of the molecular structure of complexes 6–9, and 12. (Bottom) Partially labeled
477 core for all of them. Dashed bonds show the hydrogen bonds between the –NH₂ aminated functions and
478 the coordinated azido guest.

479

480 **Figure 4.** View of the zig-zag conformation of the ring and the prismatic cavity hosting the azide anion
481 for compounds 6–9 as 12 (left), and compounds 10 and 11 (right).

482

483 **Figure 5.** View of the metallocrown and the set of hydrogen bonds (dashed bonds) that coordinate the
484 halide guests in compounds 10 and 11. Atom labeling is the same as that for compounds 6–9, and 12.

485

486 **Figure 6.** χ_{MT} vs T plot for complexes 6 (circles) and 10 (triangles). Solid lines show the best fit
487 obtained.

488

489 **Scheme 1.** Stoichiometric Relationship between Complex 1 and Complexes 6–9, as Well as 12

490

491 **Chart 3.** Prismatic Coordination of the Anionic Guests in (A) (N₃)[−] ⊂ [BT-6H⁺] Cryptand, (B)
492 Compounds 6–9 and 12, and (C) 10 and 11 (the Image to the Far Right Describes the Structural
493 Parameters Summarized in Table 2)a

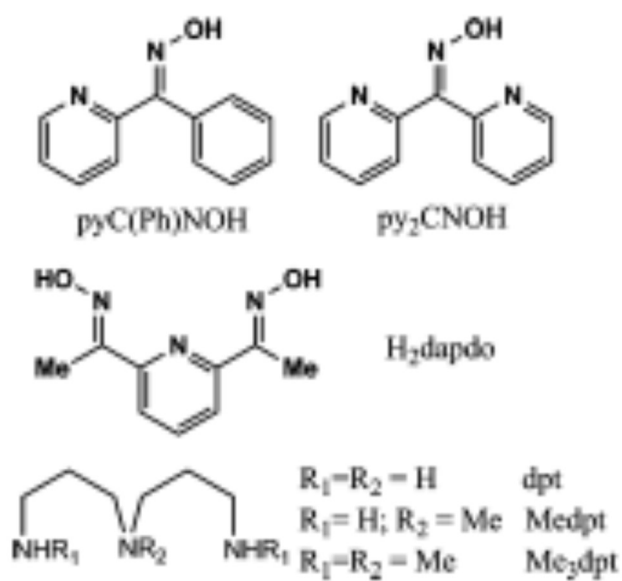
494

495 **Figure 7.** Set of hydrogen bonds promoted by the –NH₂ functions in 6–12.

496

497
498
499

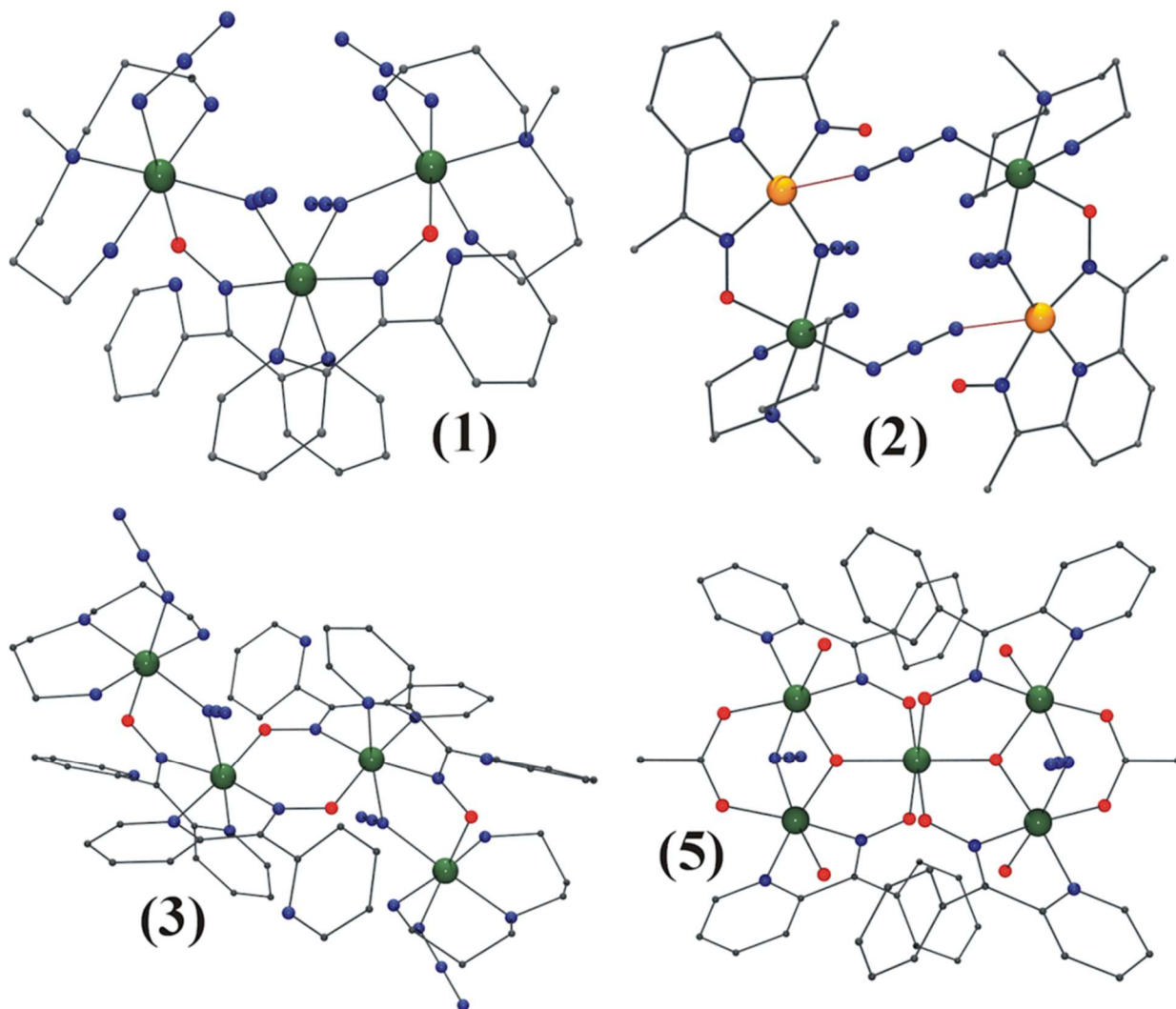
Chart 1



500
501
502
503

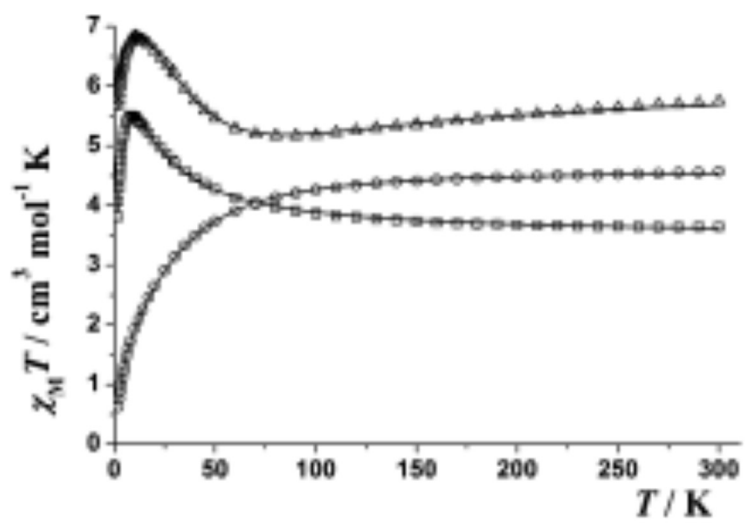
504
505
506

FIGURE 1



507
508

FIGURE 2



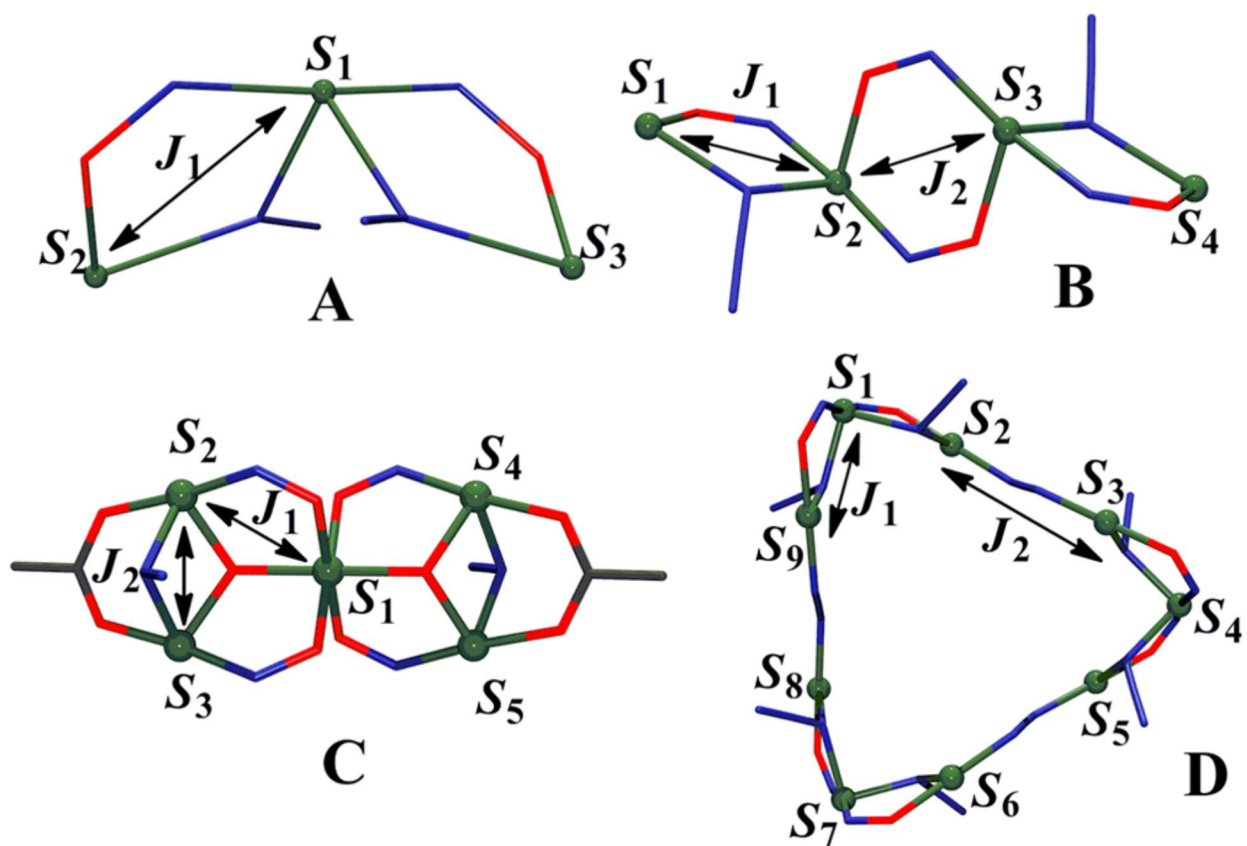
512

513

514

515
516
517

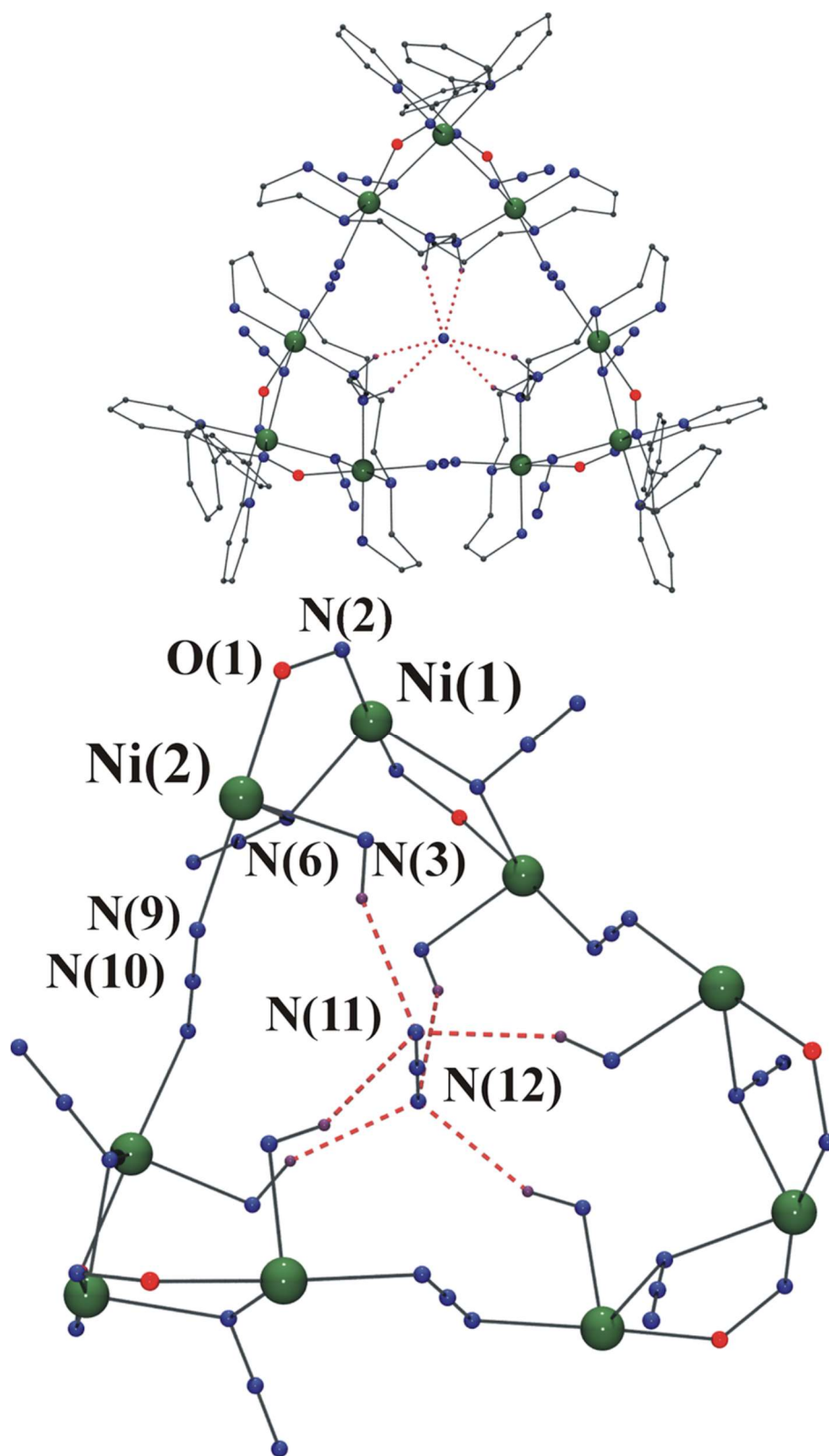
Chart 2



518
519

520
521
522

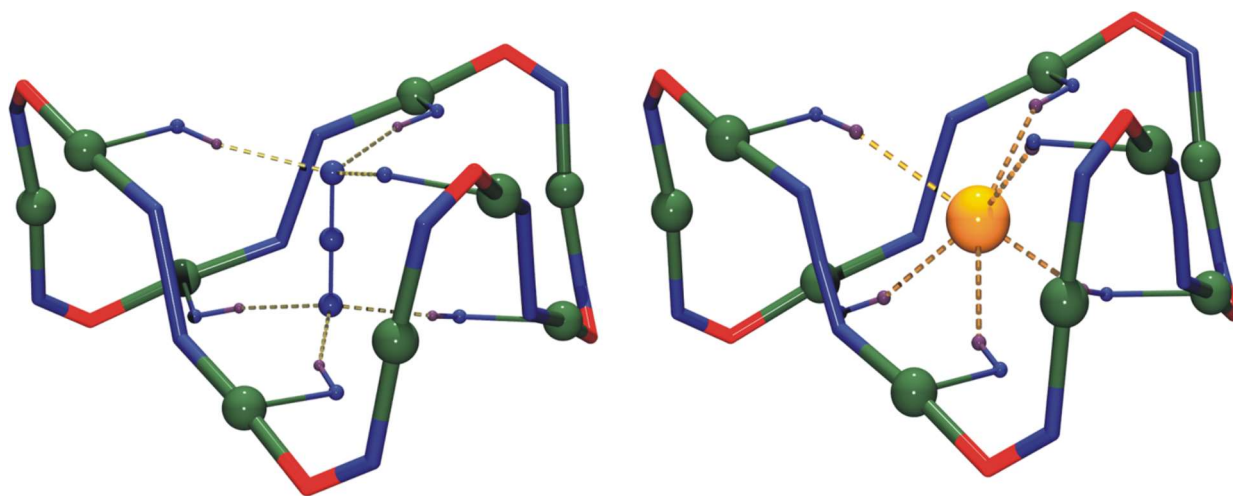
FIGURE 3



523
524

525
526
527

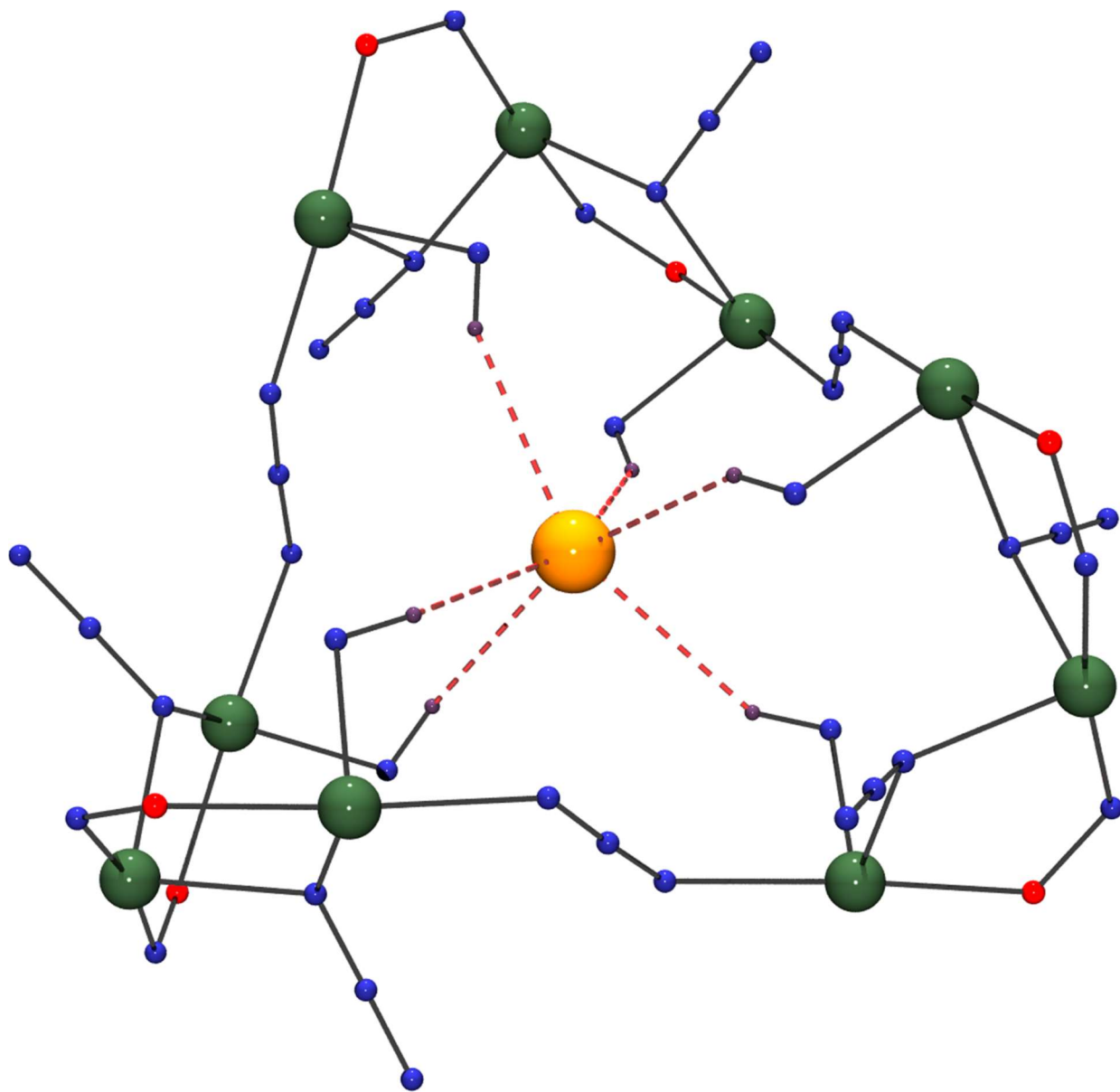
FIGURE 4



528
529

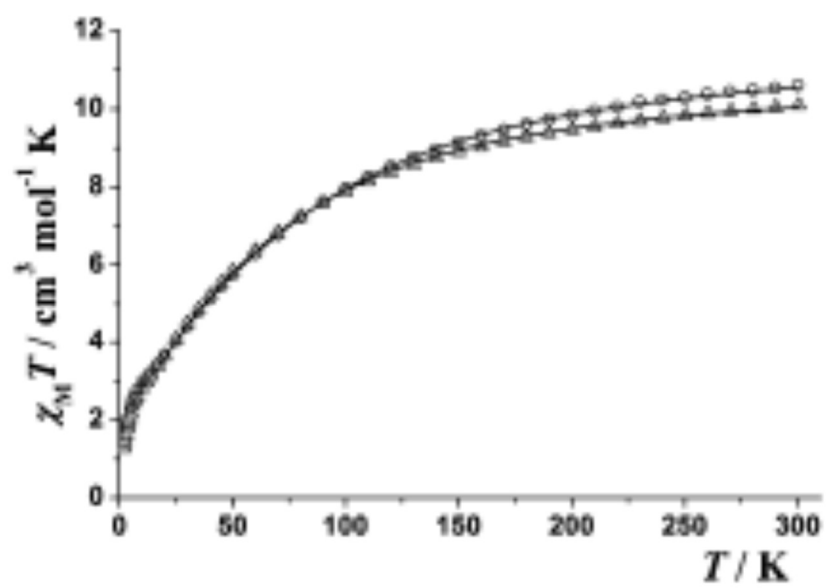
530
531
532

FIGURE 5



533
534

FIGURE 6



538

539

540
541
542

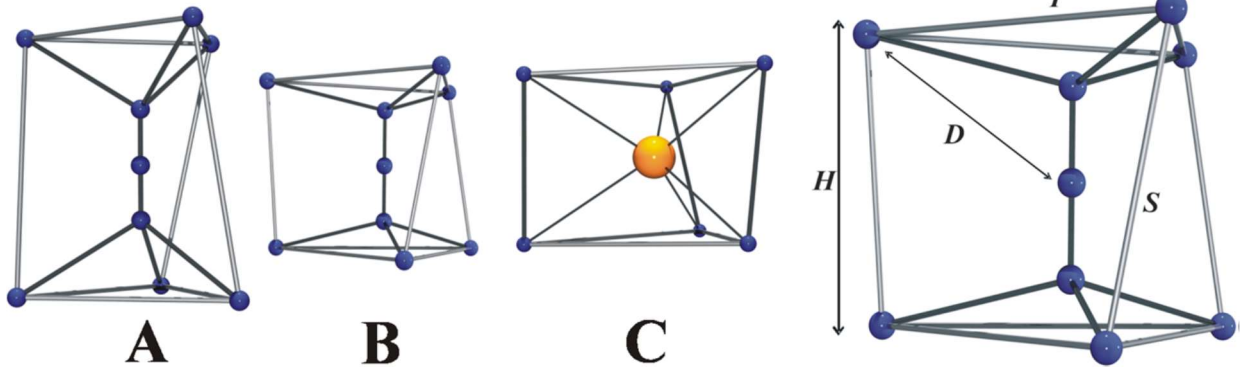
SCHEME 1



543
544
545

546
547
548

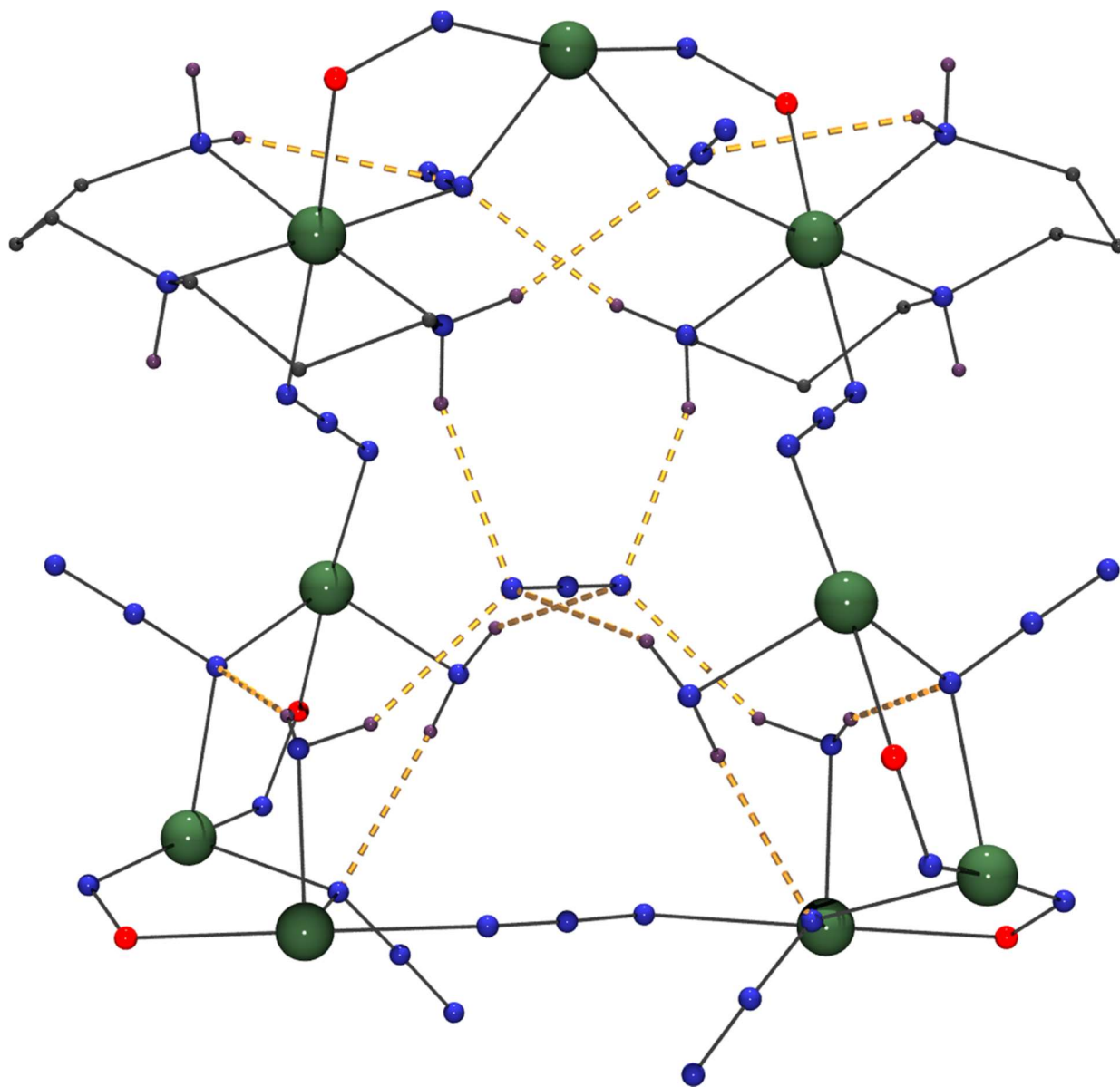
CHART 3



549
550

551
552
553

FIGURE 7



554
555
556

557 **Table 1.** Selected Interatomic Angles Related with the Azido Bridges and Oximate Torsion for
 558 Compounds 6–12
 559

compound	Interatomic Angles (deg)		
	Ni(1)–N(6)–Ni(2)	Ni(2)–N(9)–N(10)	Ni(1)–N(2)–O(1)–Ni(2)
6	110.89(7)	128.2(2)	176(2)
7	110.8(1)	127.6(2)	176(3)
8	110.9(1)	127.9(3)	173(4)
9	111.1(1)	130.0(2)	148(4)
10	111.0(1)	129.2(3)	152(4)
11	111.3(2)	129.7(4)	178(5)
12	111.1(1)	127.0(2)	186(4)

560
 561

562 **Table 2.** Comparison between [BT-6H⁺] and {Ni9} Prism Parameters

563

compound	H ^a	T	S	D ^b	N-N _{av} -N (deg)	N-H...N
6	3.933	5.022	4.013	3.552	114.98	3.037
7	3.940	5.096	4.023	3.541	113.49	3.047
8	3.954	5.149	4.025	3.570	113.23	3.083
9	3.876	5.136	3.949	3.542	114.23	3.058
12	3.994	5.086	4.064	3.551	113.12	3.048
A ^c	5.396	4.364	5.528	3.693	95.03	2.959
10	3.786	5.176	3.861	3.538		
11	3.922	5.207	4.013	3.590		
B ^{d,e}	4.226	4.580	4.922	3.390		

^aPolyhedron height measured as the distance between the centroids of the opposite triangular faces. ^bDistance from the N-donor atoms to the centroid of the cavity. ^cA = (N₃) ⊂ [BT·6H⁺]. ^dB = (Br) ⊂ [BT·6H⁺]. ^eAverage values.

564